Sustainable Mesoporous Carbons as Storage and Controlled-Delivery Media for Functional Molecules

Dipendu Saha,[†] E. Andrew Payzant,[‡] Amar S. Kumbhar,[§] and Amit K. Naskar*,[†]

[†]Carbon and Composites Group, Materials Science and Technology Division, and [‡]Chemical & Engineering Materials Division, Oak Ridge National Laboratory, Oak Ridge, Tennessee 37831, United States

[§]Institute for Advanced Materials, NanoScience and Technology, University of North Carolina at Chapel Hill, Chapel Hill, North Carolina 27599, United States

Ⓢ Supporting Information

ABSTRACT: Here, we report the synthesis of surfactant-templated mesoporous carbons from lignin, which is a biomass-derived polymeric precursor, and their potential use as a controlled-release medium for functional molecules such as pharmaceuticals. To the best of our knowledge, this is the first report on the use of lignin for chemical-activation-free synthesis of functional mesoporous carbon. The synthesized carbons possess the pore widths within the range of 2.5−12.0 nm. In this series of mesoporous carbons, our best result demonstrates a Brunauer−Emmett−Teller (BET) surface area of 418 m^2/g and a mesopore volume of 0.34 cm^3/g, which is twice the micropore volume in this carbon. Because of the dominant mesoporosity, this engineered carbon demonstrates adsorption and controlled release of a representative pharmaceutical drug, captopril, in simulated gastric fluid. Large-scale utilization of these sustainable mesoporous carbons in applications involving adsorption, transport, and controlled release of functional molecules is desired for industrial processes that yield lignin as a coproduct.

KEYWORDS: mesoporous carbon, lignin, soft-templating, drug delivery, sustainable materials
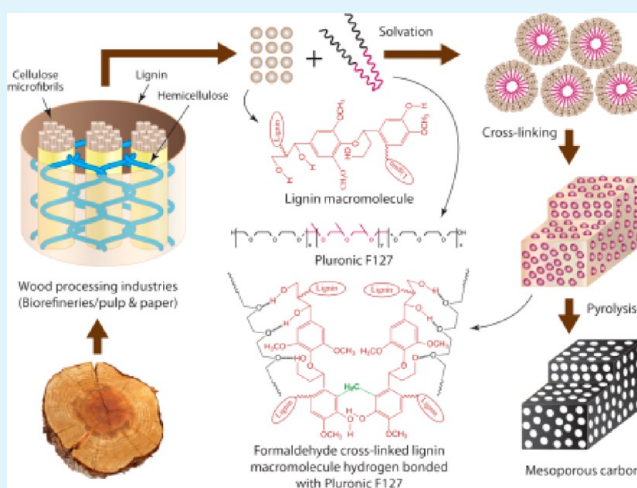
1. INTRODUCTION

Lignin has a wide range of uses, as a low-value fuel, a dispersing agent for chemicals, a modifier for polymers, and a precursor for activated carbon. Activated carbon produced from lignin does not exhibit controlled mesoporosity; usually, microporosity (pore width <2 nm) dominates in such products. Controlling pore sizes during carbon synthesis is extremely difficult, primarily because as the mass shrinks during pyrolysis, the pores collapse. An attempt to introduce controlled mesoporosity (pore width 2−50 nm) in lignin-derived carbons will facilitate various adsorption-based functionalities, including binding and release of large molecules such as dyes, pharmaceuticals, and proteins. Other than the value as sorbents, synthetic mesoporous carbons are also useful as supercapacitors, catalyst supports, membranes, and chemical sensors.[1−5]

Traditionally, mesoporous carbon has been synthesized by doping a sacrificial silica scaffold, a hard template, with a carbon precursor followed by carbonization of the precursor and subsequent removal of the template.[6] However, this is a tedious method involving corrosive and toxic chemicals, and it often yields collapsed structures upon graphitization of the resultant carbon.[7,8] More recently, a surfactant templating or "soft template" technique has been developed.[9−15] In it, mesoporous carbon is synthesized by cross-linking organic resins in the presence of some sacrificial surfactants, followed by pyrolysis, leading to removal of the surfactant and carbonization in the same step.

Amphiphilic block copolymeric surfactants form self-assembled structures of micelles as a consequence of repulsive interactions between the covalently bonded polymer segments.[16] One segment interacts with resin and forms a miscible system, while the other phase tends to form nanometer-sized immiscible domains in the precursor resin matrix. The majority of the precursors employed to synthesize mesoporous carbons are phenolic resins such as cross-linked phenol,[9−11] resorcinol,[12,13] phloroglucinol,[7,14] and hexaphenol.[15] These resins form a very strong hydrogen bond between phenolic hydroxyl groups and the miscible segment of the surfactant macromolecule. Lignin, the third most abundant natural polymer next to cellulose and chitin, contains an abundance of aliphatic and phenolic hydroxyl groups. Although lignin-based activated
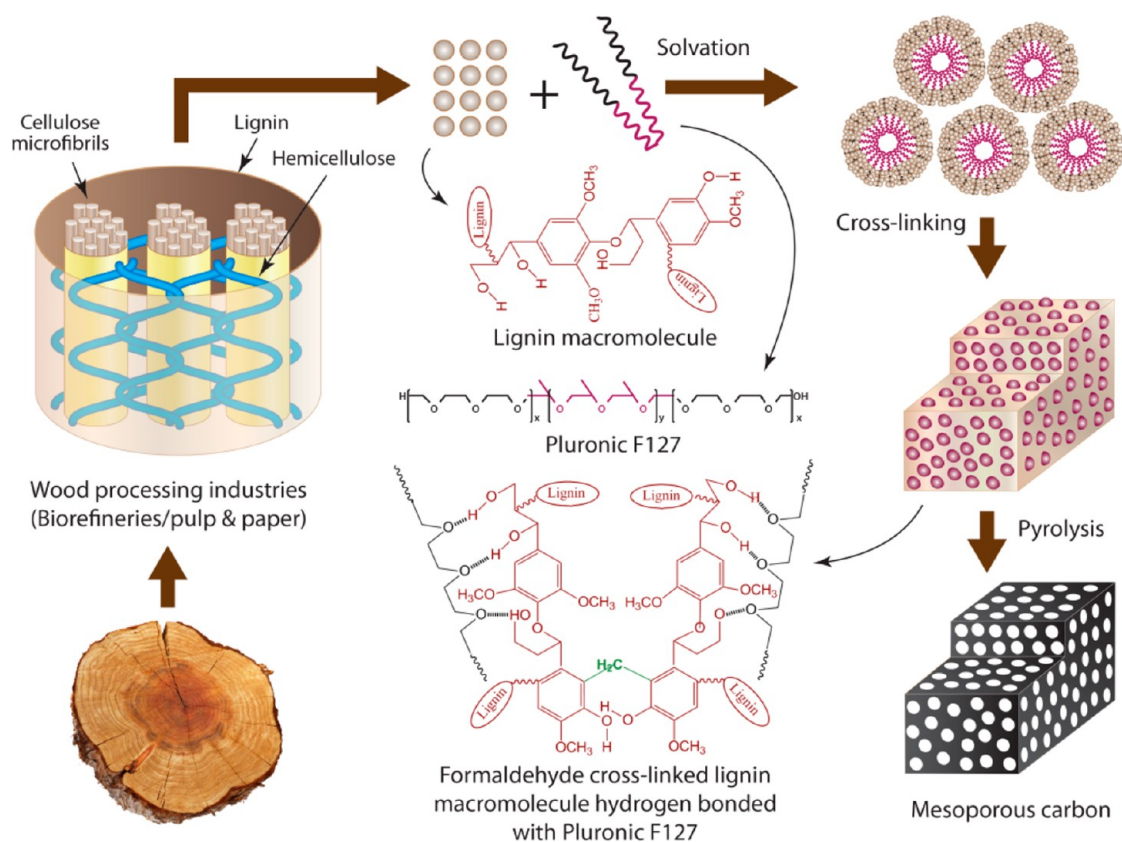
Figure 1. Schematic of mesoporous carbon synthesis from lignin.

microporous carbons are very common, it has remained an unexplored precursor for the synthesis of mesoporous carbon, perhaps because of its polydispersity, heterogeneity (aromatic—aliphatic), and hyperbranched structure.

Structurally, lignin polymers consist of three phenyl-propanoid monomers: coumaryl, guaiacyl, and sinapyl alcohols. The composition and physical characteristics of lignin depend on the plant genotype and the lignin isolation techniques.[17] The types of lignin employed in this study are the methanol-soluble fraction of an experimental Kraft-processed hardwood lignin and an acid-catalyzed pre-cross-linked derivative (condensation product) of the hardwood lignin. Here, we have presumed that the solvent-extracted lower-molecular-weight fraction of lignin provides better control over the template synthesis of carbon. In this work, we have utilized Pluronic F127 (BASF) as the surfactant. It has a typical formula[7] of $[(PEO)_x(PPO)_y(PEO)_x]$ ($x = 106$, $y = 70$) with an average molecular weight of 12 600. The PEO segment of surfactant and the hydroxyl groups of lignin form hydrogen bonding along the periphery of micelles containing PPO segments at the core (Figure 1). The overarching goal of this work was to develop utilization pathways of lignin-derived sustainable mesoporous carbons in applications involving adsorption, transport, and controlled release of functional molecules.

2. EXPERIMENTAL SECTION

All the mesoporous carbons are considered to be lignin-derived mesoporous carbons (LMCs) and are designated as LMC-1 through LMC-6. Details of the sample identities are provided in Table 1. The corresponding polymer resin before carbonization is referenced as *poly*-LMC.

Table 1. Pore Textural Characteristics of Lignin-Derived Carbons

entry	preparation (F127 content wt %)	BET specific surface area (m^2/g)	mesopore volume (cm^3/g)	total pore volume (cm^3/g)
LMC-1	HCHO/acid (105)	418	0.34	0.50
LMC-2	HCHO/acid (210)	205	0.13	0.20
LMC-3	HCHO/base (160)	222	0.15	0.22
LMC-4	HMTA/base (160)	214	0.17	0.19
LMC-5	pre-cross-linked lignin/THF (116)	208	0.24	0.28
LMC-6	pre-cross-linked lignin/DMF (116)	276	0.11	0.22

2.1. Preparation of Poly-LMC-1 and Poly-LMC-2 Samples. These mesoporous carbon samples were prepared with 5 g of methanol-soluble fractions extracted from Kraft-processed hardwood lignin. For each batch, the specific amounts of lignin and Pluronic F127 (BASF, 105 wt % and 210 wt % of lignin, surfactant was not added for LC-0) were dissolved in 40 mL of tetrahydrofuran (THF), along with 600 μL of 6 M hydrochloric acid (HCl) and stirred for several hours. Afterward, 2 mL of 37% formaldehyde was added, and the mouth of the flask was sealed tightly with a septum and stirred at 70 °C (reflux) for 5 days. [The septum on the mouth of the flask must be sealed with caution, because the reaction temperature is above the boiling point of THF (66 °C).] After the reaction time, the flask was cooled and the solution was placed on a Petri dish and dried at ambient and gradually elevated temperature to introduce evaporation-induced self-assembly.

2.2. Preparation of Poly-LMC-3 and Poly-LMC-4 Samples. These samples were prepared with 1 g of methanol-soluble fractions extracted from Kraft-processed hardwood lignin. Typically, 1 g of lignin, 0.06 g of NaOH, and 0.5 mL of formaldehyde (37%) (or 0.3 g HMTA for LMC-4) were dissolved in a mixture of 10 mL of deionized (DI) water and 20 mL of THF. The reaction mixture was stirred for 5 days at 60 °C to induce cross-linking. Afterward, the reaction mixture was cooled, concentrated using a rotovap, and mixed with 1.4 g of F127 and 1 mL of 6 M HCl in 22 mL of THF. The mixture was stirred for 24 h and dried on a Petri dish in a manner similar to that for LMC-1 and LMC-2.

2.3. Preparation of Poly-LMC-5 and Poly-LMC-6 Samples. These samples were synthesized similarly to LMC-3 and LMC-4 except for the prior cross-linking step. For acid-catalyzed pre-cross-linking, lignin was treated with excess 6 M HCl in slurry form and stirred at 90 °C inside a sealed round-bottom flask for 24 h. Later, similar solvation technique of dried precross-linked lignin with F127 was employed under acidic conditions. The pre-cross-linked hardwood lignin was employed on a 1-g basis and solvated in THF (for LMC-5) and N,N-dimethyl formamide (for LMC-6).

2.4. Carbonization. All dried samples were carbonized in a tube furnace in N_2 flow with the heating profile being heating from room temperature (RT) to 400 °C, at a rate of 1 °C/min, and then heating from 400 to 1000 °C at a rate of 2 °C/min, followed by maintenance at 1000 °C for 15 min. Afterward, the samples were cooled to near-ambient temperature in the nitrogen flow.

2.5. Characterization. The thermogravimetric analysis (TGA) of the polymer samples was performed after pretreating them at 100 °C to remove the absorbed moisture and residual solvent. The mass loss then was monitored in a Model TGA Q500 system (TA Instruments) at a heating rate of 10 °C/min up to 1000 °C under nitrogen. The pore textural properties of the mesoporous carbons were investigated by nitrogen adsorption–desorption at −196 °C (77 K) and pressure up to ambient condition in a Quantachrome Nova 2000 analyzer. The pore size distributions in the carbon samples were calculated by employing nonlocal density functional theory (NLDFT), using the data reduction software of the instrument. To reflect more light on the structures and porous moieties of this mesoporous carbon, we performed small-angle and wide-angle X-ray scattering (SAXS and WAXS) in an Anton Paar Saxess mc² instrument operated with Cu Kα radiation (λ = 1.54 Å). High-resolution secondary electron micrographs were obtained using a Hitachi Model S4800 system operating at 5 kV and 3 µA. Transmission electron microscopy (TEM) micrographs of carbon materials were obtained using a JEOL 2010F FasTEM system operating at 200 kV.

2.6. Experimental Methodologies of Drug Loading and Release Experiments. Forty milligrams (40 mg) of the LMCs were utilized for loading from an excess aqueous Captopril (Acros Organics) solution. Based on a simple thermogravimetric analysis, it was observed that the LMCs could load as high as 10 wt % Captopril on a dry mass basis. The external surface of the loaded mesoporous carbons were rinsed with pure solvent and dried in a vacuum oven at ~50 °C, and placed in 50 mL of simulated gastric fluid without pepsin (SGF; 0.2% w/v NaCl, aqueous HCl, pH adjusted to ~1.5). The mixture was maintained at ambient temperature for 48 h under mild stirring (~60 rpm) for in vitro drug release monitoring. All the drug concentrations in the media were measured by UV–vis spectroscopy in a Perkin–Elmer Lambda 900 instrument utilizing a calibration curve on absorbance at various concentrations of the drug in a SGF medium.

3. RESULTS AND DISCUSSION

In this work, we have cross-linked lignin with formaldehyde in the presence of both acid and base catalyst. To explore the alternative cross-linking chemistries, we have employed (i) hexamethylenetetramine (HMTA)-based cross-linking in the presence of base catalyst and (ii) mineral acid (HCl) catalyzed thermally precross-linked hardwood lignin. For the pre-cross-linked lignin, surfactant ratio was varied from 105% to 210%; for the rest of the samples, it was within 100%–120%. All the

mesoporous carbons were designated as LMC-1 through LMC-6 (lignin-derived mesoporous carbon). The details of the samples identities are provided in Table 1. The corresponding polymer resin before carbonization is referred to as poly-LMC. To understand the effect of surfactant in generating the mesopores, a control without surfactant (LC-0) was prepared. In addition, to investigate the role of surfactant micelles in the porosity of resulting carbon, we used nonsurfactant poly-ethylene oxide homopolymer (M_w = 13 800, Sigma−Aldrich) in two varying proportions (100% and 200% surfactant to lignin).

All of the *poly*-LMC samples begin to decompose at temperatures beyond 200 °C with prominent weight loss that is due to the removal of surfactant. The effective carbon yield in *poly*-LMCs (20%−30%, based on lignin content) is lower than that observed in a pure lignin−formaldehyde cross-linked sample (45%) with no surfactant (see Figure S1 in the Supporting Information). The derivative plots from thermogravimetric analysis (TGA) (Figure 2) show that the peak
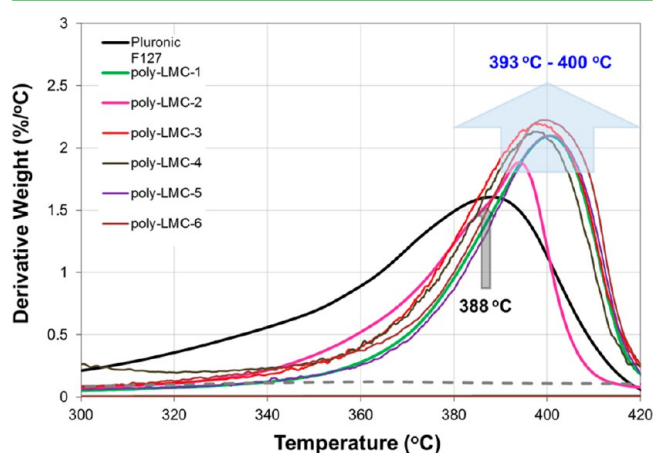

Figure 2. Derivative thermogravimetric plots of precursors of mesoporous carbon along with Pluronic F127, showing the elevation of decomposition temperatures of Pluronic F127 in poly-LMC samples.

maximum temperatures for the decomposition of surfactant are shifted toward higher temperature for *poly*-LMCs, because of enhanced lignin−surfactant interaction (hydrogen bonding). The manifestation of stable self-assembly of surfactant-doped cross-linked lignin precursor materials can be further illustrated in the following sections through characterization of pore texture in their carbonized derivatives.

The adsorption−desorption isotherms of nitrogen at 77 K (−196 °C) for the LMC samples (Figure 3a) are Type IV, according to the IUPAC nomenclature,[18] and the hysteresis loops confirm the presence of mesoporosity. The Brunauer−Emmett−Teller (BET) specific surface areas are within a range of 418−205 m^2/g. The detailed pore textural characteristics are provided in Table 1. The differential pore size distribution calculated by nonlocal density functional theory (Figure 3b) depicts that the mesopore volume occupies the pore widths within the range of 2.5−12.0 nm. The cumulative pore volume data of LMC samples are shown in Figure 3c.

The carbon obtained from lignin−formaldehyde cross-linked resin, without the surfactant (LC-0), yields low BET specific surface area (36 m^2/g) and pore volume (0.036 cm^3/g). Thus, surfactant plays an effective role in creating the porous moieties within the carbon matrix. A better pore texture in LMC-1
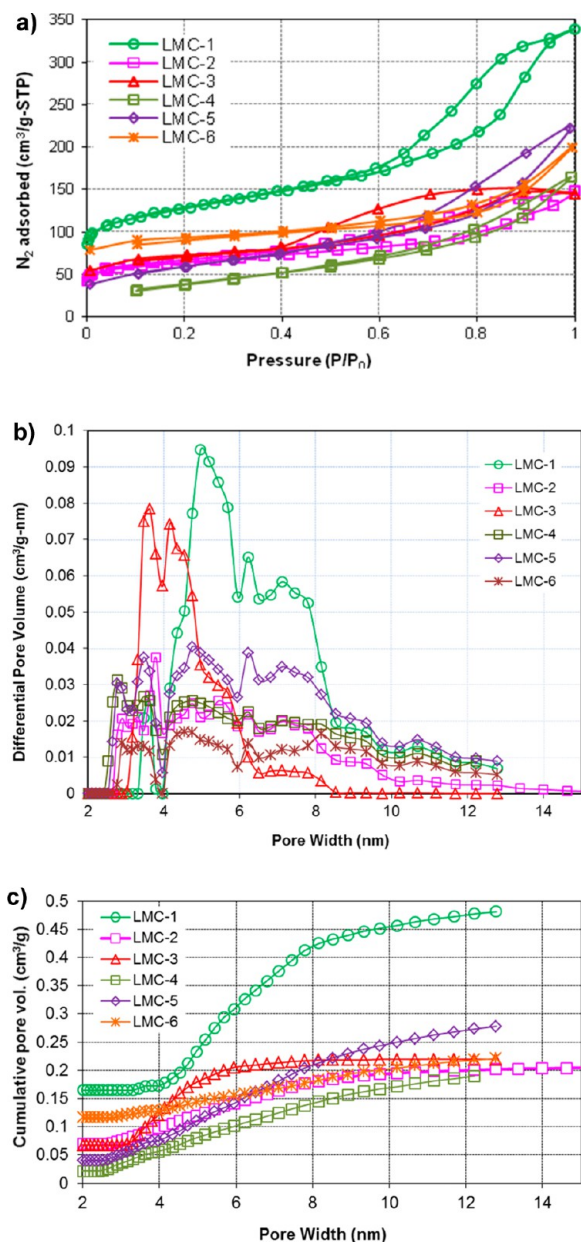
Figure 3. (a) N_2 adsorption−desorption plots of LMC-1 through LMC-6 at 77 K. (b) Pore size distribution of LMC samples calculated via the NLDFT method from N_2 adsorption−desorption plots. (c) Cumulative pore size distributions of LMC-1 through LMC-6 calculated via the NLDFT method from N_2 adsorption−desorption plots at 77 K.

compared to LMC-2, which were synthesized similarly with different surfactant ratios, suggests that a very high surfactant content makes surfactant-swollen cross-linked lignin as dispersed domains in the soft surfactant matrix, which collapses during thermal pyrolysis. Therefore, compositions wherein lignin molecules fail to create a continuous matrix for surfactant domains give low porosity. LMC-3 and LMC-4, which are cross-linked in base medium prior to solvation in a separate step usually demonstrated a lower porosity than LMC-1. This suggests that the initial hydrogen bonding of lignin with surfactant prior to cross-linking helps to maintain better structural domain that contributes to the higher porosity. LMC-5 and LMC-6 are very similar to LMC-3 and LMC-4,

except lignin was cross-linked during isolation and, hence, did not require a prior cross-linking step. In this method, however, based on proper solvent selection and the swelling condition of the cross-linked lignin matrix, the surfactant could penetrate and form micelles. To understand whether or not the formation of micelles through surfactant is critical for mesoporosity in the resulting carbon, we have used nonsurfactant PEO homopolymer (of similar molecular weight to Pluronic F127) in cross-linked lignin matrix. The carbon from lignin/PEO blends prepared under identical conditions yields low porosity with BET specific surface area of 48 m^2/g and total pore volume of 0.023 cm^3/g. Thus, micelle formation is critical for the synthesis of mesoporous carbon from lignin.

To date, lignin has been ignored as a candidate for synthesis of templated mesoporous carbon, perhaps because of the availability of other synthetic precursors that yield excellent mesopore texture. For example, Deng et al.[19] synthesized mesoporous carbon from phenolic resole with PEO-b-PS as surfactant, and it yielded a total pore volume of 0.47−0.63 cm^3/g, with ∼50% micropore content. Similar resin with triblock copolymer surfactant[20] yields BET surface area as high as 1490 m^2/g with nearly 50% contribution from micropores (720 m^2/g) in carbon. Lee and Oh[12] synthesized resorcinol-derived mesoporous carbon that demonstrated BET surface area of 378−569 m^2/g with pore widths of 1.0−50.1 nm. Liang and Dai[7] obtained a similar BET surface area with narrower pore widths (5.4−9.5 nm) in an ordered mesoporous carbon from phloroglucinol.

An exact and thorough comparison of mesopore texture in our synthesized carbon with that of current state-of-the-art mesoporous carbons from synthetic precursors is difficult. This is due to (1) the lack of detailed reports on specific mesopore percentage in total pore volume in many published articles and (2) the unavailability of uniform, monodisperse, and standard lignin polymer. Industrially available lignin has wide molecular weight distribution, which likely causes wide pore-size distribution in the synthesized carbon. Nevertheless, in terms of quality, our material LMC-1 is comparable to the majority of surfactant-templated mesoporous carbons made from synthetic precursors. Thus, this work offers an inherent advantage of introducing lignin, a material from renewable resources, as the sustainable precursor for mesoporous carbons.

To understand the structures of porous moieties in this mesoporous carbon, we have performed small-angle and wide-angle X-ray scattering (SAXS and WAXS). The scattering patterns are shown in Figure 4. The broad (002) peak appears due to the disordered carbon layers in all the samples. A small response within the Q-values of 0.1−0.5 Å^{-1} was observed in all the patterns, but it was more prominent in LC-0. Such a response can be attributed to the smaller pores (micropores) of carbon-based material, and the smoother pattern in the low-Q region is representative of the larger (meso/macro) porosity.[21,22] Further analysis of the SAXS pattern were made on the basis of approximation of homogeneous distribution of pores in carbon matrix and by employing an empirical model developed by Kalliat et al.[21] and later modified by Gibaud et al.[22,23] The results of the empirical model fitting are shown in the Supporting Information. Although the SAXS model fitting data (see Table S1 and Figures S2(a)−(c) in the Supporting Information) support decreased mesoporosity from LMC-1 to LMC-2, it indicates an increase in small-pore density in LC-0 and contradicts the adsorption-based data. It suggests a possible generation of closed microporosity in LC-0 that became
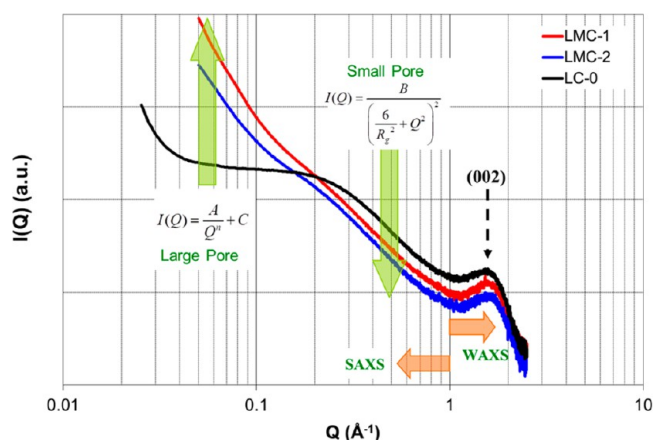
Figure 4. Small-angle and wide-angle X-ray scattering (SAXS and WAXS) of LMC-1, LMC-2, and LC-0.

Figure 5. Representative (a) scanning electron microscopy (SEM) micrograph and (b) transmission electron microscopy (TEM) micrograph of LMC-1 sample.

invisible to the gas adsorption studies. Such microporosity, along with poor graphitic crystal structure, leads to poor strength and brittleness in the lignin-derived carbon.

The texture of the synthesized carbon is further supported by electron micrographs of the lignin-derived carbons and shown in the Supporting Information. In Figure 5, the SEM image consistently indicates that macroscopic roughness on the surface of LMC-1 is caused by the fugitive micelles of surfactants in the precursor matrix. The implication is that macropores with significant surface roughness originated within the macrostructure of the carbon and that the micro/mesopores are situated within the microscopic domains of these structures, although not visible within the given magnification of the SEM image. As shown in Figure S3 in the Supporting Information, on the other hand, the surface of LC-0 seems to be quite smooth and glassy, suggesting the absence of open pores in the carbon matrix. The representative TEM image (Figure 5b) confirms the presence of porosity in the microscopic domains of LMC-1, without the pores having any visible structural order. The microscopic domains of LC-0 (Figure S3 in the Supporting Information) seem to be quite smooth and do not reflect any substantial porosity, compared to its surfactant-templated counterpart.

The mesoporosity in our synthesized porous carbons is intended to be used for applications relevant to the adsorption−desorption kinetics of large functional molecules that can fit in those pores. Earlier, mesoporous inorganic materials were shown to be useful for controlled and targeted drug delivery systems.[24] The key advantages of employing a mesoporous material as drug release media are 2-fold: (1) it can confine a sufficient quantity of a poorly soluble drug within its porous moiety at a molecular level (through physisorption), thereby negating its crystallization energy; and (2) it allows controlled release of the drug molecules though desorption and diffusion from its pores at the therapeutic level for a sustained interval of time. This process leads to minimal premature release and eliminates the possibility of an ineffective sawtooth profile of drug concentration exceeding the level of toxicity at prolonged and intense drug exposure.[25] In this work, we have demonstrated LMC-1 and LMC-2 as excellent release media for a representative drug, Captopril, which is used as an angiotensin-converting enzyme (ACE) inhibitor and prescribed for the treatment of hypertension and a certain class of congestive heart failure.
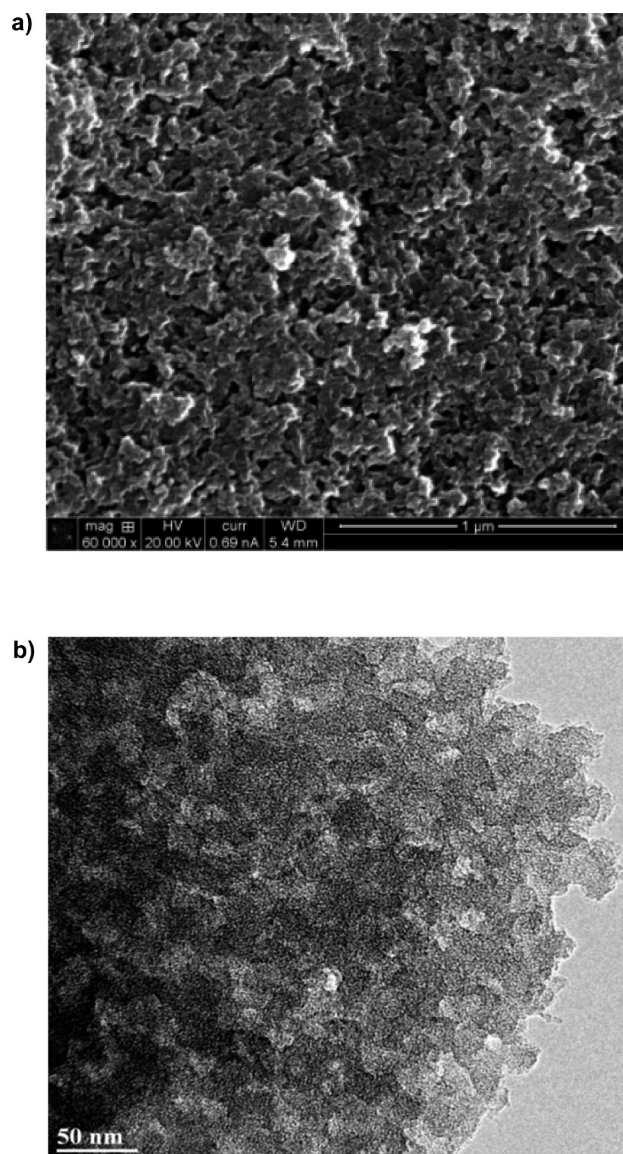
Figure 6 shows the captopril release profile under an examination time of 48 h. The pattern suggests that both LMC samples could well control the release of the drug over a prolonged time. It is observed that 60%−70% of the drug was released rapidly within an exposure time of 3−4 h, after which the release profile plateaued, suggesting a reduced amount released in the later period. Higuchi kinetic analysis,[26,27] shown in the inset of Figure 6, also confirms two different regimes of drug release, giving two possible release constant values. For LMC-2, at the onset of slow desorption kinetics, the quantity of released drug deviates significantly from the fast-release, linear kinetic data passing through the origin. Analysis by the Korsmeyer−Peppas equation[28] provides the release rate constant value and order of release kinetics for the valid data within the first 60% of total drug release. An analysis of the release data based on the Korsmeyer−Peppas equation is provided in the Supporting Information. An attempt to load Captopril onto LC-0, which is the control carbon material with the least porosity, yielded no result. It is believed that the lack
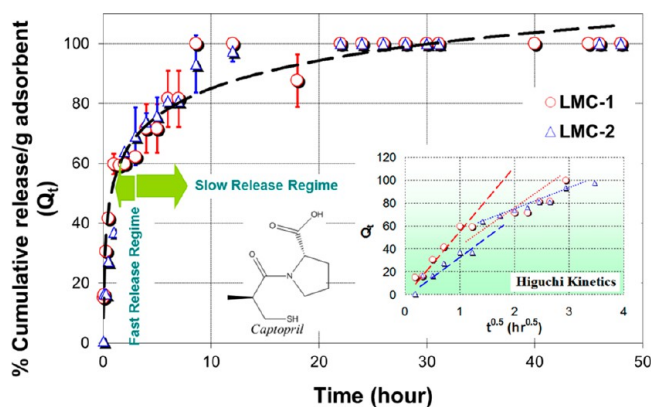
Figure 6. Release of Captopril from LMC-1 and LMC-2 in simulated gastric fluid (SGF).

of appropriate porosity in the carbon caused no sorption of drug; therefore, a study of drug release kinetics from control nonporous monolith carbon (LC-0) was irrelevant.

The presence of fast and slow regimes in the drug release profiles is quite ubiquitous in porous-media-based drug delivery systems.[29,30] For mesoporous silica, these two regimes were explained by the partial solubility of silica in the dissolution media and by the pore size effect.[28] In our study, dissolution of carbon media can be ruled out; the only controlling influence is the pore geometry effect that influences Fickian diffusion (for slow stirring, the turbulence effect can be neglected). It can be fairly hypothesized that the drug molecules present near the pore mouth experience the least sorption potential and a shorter path of diffusion resistance. Therefore, those can be released in the fastest interval of time; drugs located deep inside the pore experience stronger absorption potential and require a longer time to become completely desorbed.

As the majority of carbon-based materials possess varying pore widths, a wider pore would provide a weak adsorptive potential, compared to a narrower pore, and hence would allow the drug molecules to escape early. It can also be hypothesized that a same-sized tortuous pore will present more resistance in the path of diffusion than a straight pore, thereby making release of the drug more difficult. Although all of these effects can share the responsibility of creating two different regimes of release, a series of controlled experiments with more ordered materials is currently ongoing to confirm these hypotheses on fast and slow regions of drug diffusion.

Activated carbons have been used extensively for adsorptive removal of drug overdose and snake venom removal.[31] Also, porous carbon has been successfully employed for medicinal application without any evidence of toxicity to human physiology.[32] The bioactivity study of nanoscale carbon particles such as nanotubes is reportedly affected by the residual transition metals used for nanocarbon synthesis.[33] Recent study reveals that purified and prefunctionalized carbon nanotube's high surface area can be exploited for successful drug loading and delivery.[34] Although the mesoporous carbon monolith studied here are significantly different from nano-carbon materials, it is anticipated that these material will be harmless when used as drug carrier. A detailed study with an animal model was beyond the scope of this work.

4. CONCLUSIONS

In conclusion, we have successfully synthesized surfactant-templated mesoporous carbon from a sustainable precursor, lignin, which, to the best of our knowledge, until now, has been used only for the synthesis of activated carbon, not controlled mesoporous carbon. One of our mesoporous carbons has a BET surface area of 418 m^2/g and mesopore volume of 0.34 cm^3/g; the carbons also exhibit characteristic mesopores at a volume 2−6 times that of the micropores. This carbon has successfully demonstrated the controlled release of an ACE-inhibitor drug, captopril. This suggests the potential use of lignin-based mesoporous carbon as unique sustainable functional carbon materials for controlled drug delivery. Because of their potential to adsorb large molecules in mesopores, these materials also will be useful for pollution control, dye adsorption, protein binding, molecular transport and catalysis, and other controlled-release applications for specialty chemicals. Successful utilization of the mesoporous carbon synthesized from lignin will not only reduce the cost of material and contribute to sustainability through use of a natural product but will also influence the economy of lignin-producing industries. It broadens the scope of lignin consumption in significantly high-value product forms.

■ ASSOCIATED CONTENT

$\textbf{S}$ Supporting Information

Supporting information for this article on the thermal analysis of the precursor, pore analysis of the carbons by small-angle X-ray scattering and model fitting data, electron microscopy of control sample and the drug release kinetic equations is available. This information is available free of charge via the Internet at http://pubs.acs.org.

■ AUTHOR INFORMATION

Corresponding Author
*Fax: (+) 1 865 574 8257. E-mail: naskarak@ornl.gov.

Notes
The authors declare no competing financial interest.

■ ACKNOWLEDGMENTS

■ REFERENCES

(1) Lee, J.; Yoon, S.; Hyeon, T.; Oh, S. M.; Kim, K. B. *Chem. Commun.* **1999**, 2177−2178.
(2) Harada, T.; Ikeda, S.; Miyazaki, M.; Sakata, T.; Mori, H.; Matsumura, M. *J. Mol. Catal. A* **2007**, *268*, 59−64.
(3) Lee, D.; Lee, J.; Kim, J.; Kim, J.; Na, H. B.; Kim, B.; Shin, C.-H.; J. Kwak, H.; A. Dohnalkova, A.; Grate, J. W.; Hyeon, T.; Kim, H. S. *Adv. Mater.* **2005**, *17*, 2828−2833.
(4) Vinu, A.; Streb, C.; Murugesan, V.; Hartmann, M. *J. Phys. Chem. B* **2003**, *107*, 8297−8299.
(5) Saha, D.; Deng, S. *J. Colloid Interface Sci.* **2010**, *345*, 402−409.
(6) Ryoo, R.; Joo, S. H.; Jun, S. *J. Phys. Chem. B* **1999**, *103*, 7743−7746.

5873

dx.doi.org/10.1021/am401661f | *ACS Appl. Mater. Interfaces* 2013, 5, 5868−5874

(7) Linag, C.; Dai, S. *J. Am. Chem. Soc.* **2006**, *128*, 5316−5317.

(8) Saha, D.; Deng, S. Self-Assembled Ordered Mesoporous Carbon: Synthesis, Characterization and Applications. In *Activated Carbon: Classifications, Properties and Applications*; Nova Science Publishers: New York, 2011; Invited chapter, pp 509−538.

(9) Meng, Y.; Gu, D.; Zhang, F.; Shi, Y.; Yanf, H.; Li, Z.; Yu, C.; Tu, B.; Zhao, D. *Angew. Chem., Intl. Ed.* **2005**, *44*, 7053−7059.

(10) Fang, Y.; Gu, D.; Zou, Y.; Wu, Z.; Li, F.; Che, R.; Deng, Y.; Tu, B.; Zhao, D. *Angew. Chem., Intl. Ed.* **2010**, *49*, 7987−7991.

(11) Zhang, F.; Meng, Y.; Gu, D.; Yan, Y.; Yu, C.; Tu, B.; Zhao, D. *J. Am. Chem. Soc.* **2005**, *127*, 13508−13509.

(12) Lee, K. T.; Oh, S. M. *Chem. Commun.* **2002**, 2722−2723.

(13) Tanaka, S.; Nishiyama, N.; Egashira, Y.; Ueyama, K. *Chem. Commun.* **2005**, 2125−2126.

(14) Saha, D.; Deng, S. *Langmuir* **2009**, *25*, 12550−12560.

(15) Saha, D.; Contescu, C. I.; Gallego, N. C. *Microporous Mesoporous Mater.* **2012**, *155*, 71−74.

(16) Balsara, N. P.; Tirrell, M.; Lodge, T. P. *Macromolecules* **1991**, *24*, 1975−1986.

(17) Boudet, A. M.; Kajita, S.; Grima-Pettenati, J.; Goffner, D. *Trends Plant Sci.* **2003**, *8*, 576−581.

(18) Sing, K. S. W.; Haul, R. A. W.; Moscou, L.; Pierotti, R. A.; Rouquerol, J.; Siemieniewska, T. *Pure Appl. Chem.* **1985**, *57*, 603−619.

(19) Deng, Y.; Cai, Y.; Sun, Z.; Gu, D.; Wei, J.; Li, W.; Guo, X.; Yang, J.; Zhao, D. *Adv. Funct. Mater.* **2010**, *20*, 3658−3665.

(20) Meng, Y.; Gu, D..; Zhang, F.; Shi, Y.; Cheng, L.; Feng, D.; Wu, Z.; Chen, Z.; Wan, Y.; Stein, A.; Zhao, D. *Chem. Mater.* **2006**, *18*, 4447−4464.

(21) Kalliat, M.; Kwak, C. Y.; Schmidt, P. W. Small-Angle X-ray Investigation of Porosity in Coals. In *New Approaches in Coal Chemistry*; American Chemical Society: Washington, DC, 1981; pp 3−22.

(22) Gibaud, A.; Xue, J. S.; Dahn, J. R. *Carbon* **1996**, *34*, 499−503.

(23) Laudisio, G.; Dash, R. K.; Singer, J. P.; Yushin, G.; Gogotsi, Y.; Fisher, J. E. *Langmuir* **2006**, *22*, 8945−8950.

(24) Vallet-Regi, M.; Balas, F.; Across, D. *Angew. Chem., Intl. Ed.* **2007**, *46*, 7548.

(25) Edlund, U.; Albertson, A. C. *Adv. Polym. Sci.* **2002**, *157*, 67−112.

(26) Highuchi, T. *J. Pharm. Sci.* **1961**, *50*, 874−875.

(27) Highuchi, T. *J. Pharm. Sci.* **1963**, *52*, 1145−1149.

(28) Korsmeyer, R. W.; Gurny, R.; Doelker, E. M.; Buri, P.; Peppas, P. A. *Intl. J. Pharm.* **1983**, *15*, 25−35.

(29) Anderson, J.; Rosenholm, J.; Areva, S.; Linden, M. *Chem. Mater.* **2004**, *16*, 4160−4167.

(30) Qu, F.; Zhu, G.; Huang, S.; Li, S.; Qiu, S. *ChemPhysChem* **2006**, *7*, 400−406.

(31) Cooney, D. *Activated Charcoal: Antidote, Remedy, and Health Aid*; TEACH Services, Inc.: Brushton, NY, 1999.

(32) Buckley, N. A.; Whyte, I. M.; O'Connell, D. L.; Dawson, A. H. *Clin. Toxicol.* **1999**, *37* (6), 753−757.

(33) Liu, X.; Gurel, V.; Morris, D.; Murray, D.; Zhitkovich, A.; Kane, A. B.; Hurt, R. H. *Adv. Mater.* **2007**, *19*, 2790−2796.

(34) Liu, Z.; Sun, X.; Nakayama-Ratchford, N.; Dai, H. *ACS Nano* **2007**, *1* (1), 50−56.